13th World Conference on Earthquake Engineering
Vancouver, B.C., Canada
August 1-6, 2004
Paper No. 1624

GENERATION OF SYNTHETIC ACCELEROGRAMS AND STRUCTURAL RESPONSE USING DISCRETE TIME MODELS

Simon ÓLAFSSON [1] and Ragnar SIGBJÖRNSSON [2]

SUMMARY

Discrete time series representation for some commonly used relations in earthquake engineering and engineering seismology are presented and the advantages compared with their continuous time counterparts are discussed. Seismic source models for simulation of ground motion based on Brune's models are presented in discrete time form as well as model of Savage-Haskell type including directivity. The discrete time models are presented as a series of recursive filters (ARMA models) that simplifies the simulation process and do not involve the numerical Fourier transform. The source models are presented as amplitude Fourier spectra. Corresponding discrete transfer functions, formulated as z-transforms, are derived that give similar response as the original continuous time transfer functions. The problem of minimising the modelling error favours models that are parameterised based on physical information, as in the case of the source models. However, this often calls for more modelling effort and is the main reason that the easier to use black-box models are often chosen instead. A discrete time site amplification model for vertically propagating S-waves is discussed. This model provides good physical insight into the problem of site amplification and facilitates estimation of site characteristics from recorded ground motion. Furthermore, a discrete time model of an SDOF-system is presented and a demonstration is made of its use for the computation of response spectra.

INTRODUCTION

The stochastic approach for simulating acceleration records for structural response studies has been practiced for several decades. Housner found that, by adding a large number of sine waves with random phase, acceleration record could be generated that had similar spectral characteristics as recorded ground motion. Later the simulation process was improved by passing white noise though a SDOF linear filter (see Housner[1] and Tajimi [2]). Furthermore, Hanks and McGuire [3] and Boore [4] demonstrated that representing the ground motion as band-limited white noise with spectra according to Brune's model [5,

[1] Senior scientist, University of Iceland, Earthquake Engineering Research Centre, 800 Selfoss, Iceland. E-mail: simon@hi.is
[2] Professor, University of Iceland, Earthquake Engineering Research Centre, 800 Selfoss, Iceland. E-mail: Ragnar.Sigbjornsson@afl.hi.is

6] gave good agreement with recorded ground motions. Their models are of the following type (see for example Change et al. [7]):

$$A(\omega) = \omega^2 B(\omega) \cdot G(\mathrm{R}) \cdot E(\omega) \cdot S(\omega) \tag{1}$$

where $A(\omega)$ is the Fourier spectrum of acceleration, ω is the frequency, $B(\omega)$ is the omega squared source model, $G(\mathrm{R})$ is the geometrical spreading function, $E(\omega)$ is the exponential spectral decay term and $S(\omega)$ represents site amplification. This model can be used for simulation by using the Eq.(1) to represent a filter. The simulated acceleration can be obtained by using band-limited white noise as input into the filter. In the following the main emphasis will be on constructing discrete time filter to simulate ground motion. Usually an envelope function is also applied to the simulated time series to account for the change in variance with time.

The main purpose of this paper is to demonstrate the formulation of the type of model represented by Eq.(1) as discrete time series models, parametric models or simply ARMA models. These type of models can also be applied as black-box models i.e. not based on the physics of the earthquake process. These type of models have been applied to strong-motion modelling by several researchers (see, for instance, Conte et al. [8]; Ólafsson and Sigbjörnsson [9]); The parametric time series model approach has also been applied to system identification in structural dynamics (see, for example, Imai et al. [10]; Celebi and Safak [11]) and are called ARMAX models when the input signal is measurable, where the X stands for exogenous (excitation or input signal).

DISCRETE TIME MODELS

A stationary stochastic process, sampled at regularly spaced time intervals may be represented by an ARMA model (see, for example, Rabiner and Gold [12]; Marple [13]; Ljung [14]), which is in fact a difference equation or a digital filter:

$$x(k) = -a_1 x(k-1) - \ldots - a_p x(k-p) + w(k) + b_1 w(k-1) + \ldots + b_q w(k-q) \tag{2}$$

where, $w(k)$ is a zero mean 'white' (Gussian) noise process with finite standard deviation, σ_w, a_1, ..., a_p and b_1, ..., b_q are the model parameters, the AR and MA parameters, respectively. Here $x(kT_\mathrm{S})$ represents a sampled version of the process $x(t)$ for k =1, 2, ..., N, where T_S is the sampling interval. In what follows the time index will be scaled for convenience so that the sampling interval is T_S = 1. The z-transform of $x(k)$ is defined as follows, where $z = \exp(j2\pi f T_\mathrm{S})$:

$$X(z) = \mathrm{Z}(x(k)) = \sum_{k=-\infty}^{k=\infty} x(k) z^{-k} \tag{3}$$

The power spectral density can be written in terms of the model parameters as:

$$P_x = T_\mathrm{S}\sigma_w^2 \left| \frac{1 + b_1 \mathrm{e}^{-j2\pi f T_\mathrm{S}} + b_2 \mathrm{e}^{-j4\pi f T_\mathrm{S}} + \ldots. + b_q \mathrm{e}^{-j2q\pi f T_\mathrm{S}}}{1 + a_1 \mathrm{e}^{-j2\pi f T_\mathrm{S}} + a_2 \mathrm{e}^{-j4\pi f T_\mathrm{S}} + \ldots. + a_p \mathrm{e}^{-j2p\pi f T_\mathrm{S}}} \right|^2 \tag{4}$$

and is evaluated over the range $-1/2T_\mathrm{S} \leq f \leq 1/2T_\mathrm{S}$.

The order of ARMA models that are to be applied are usually not known in advance. Several methods are available for order determination and parameter estimation based on second order statistics [14, 15]. These methods have also been developed to estimate time varying parameters (for example, Haykin [15]). Some commercially available parameter estimation software is also available [16]. There have also been several methods developed to estimate parameters based on higher-order statistics to handle non-linear systems where the driving noise is non-white (Swami et al. [17]; Chrysostomos [18]). The advantage of using higher-order statistics is that the phase information is preserved.

Several researchers have applied low-order ARMA models to ground-motion acceleration (see, for example, [8, 9]). As an example, the ARMA(4,1) for acceleration induced by Icelandic earthquakes is given as (Ólafsson [19]).

$$x(k) = +3.6x(k-1) - 5.11x(k-2) + w(k) + 0.99w(k-1) \tag{5}$$

Figure 1 shows the input time series (white noise) the simulated acceleration, the pole-zero plot and the theoretical and simulated spectra.

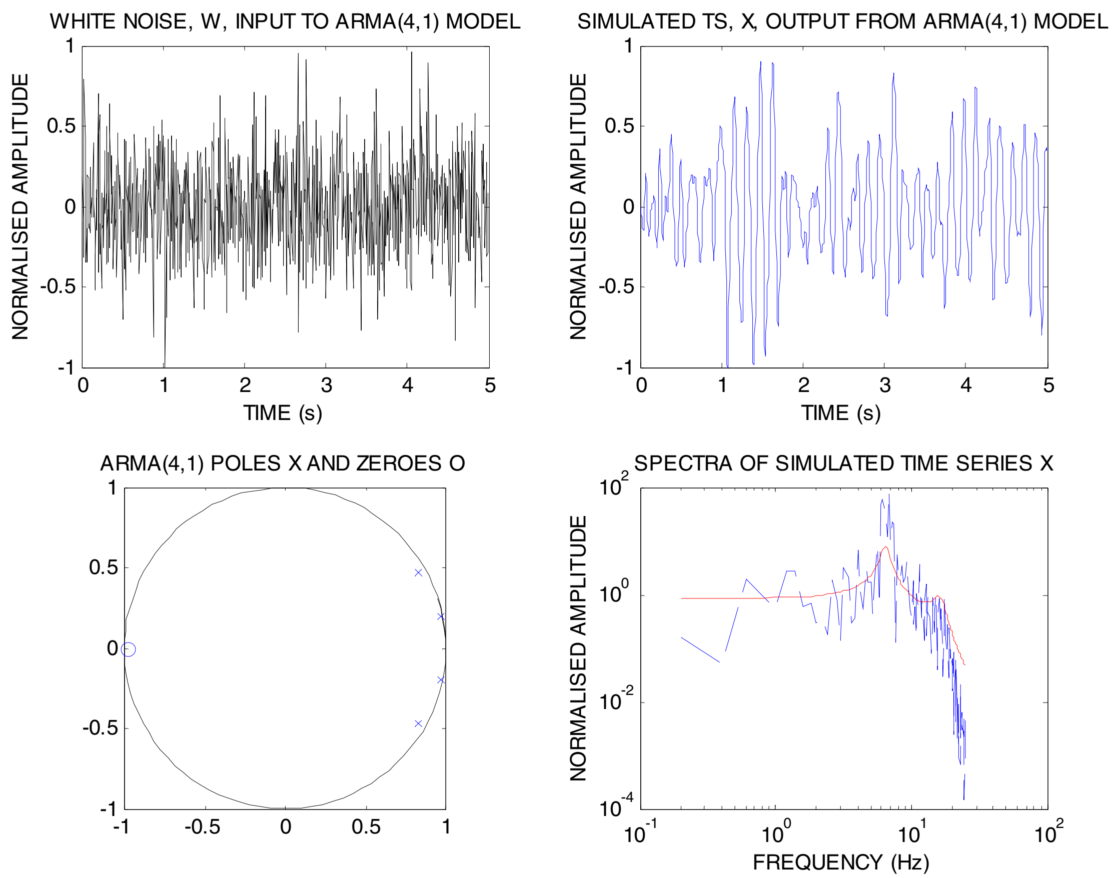

Figure 1: Simulated acceleration using ARMA(4,1) model. The figure shows a plot of the input to the ARMA filter, a white noise sequence, $w(k)$; the output of the ARMA filter (acceleration time series, $x(k)$) and the spectrum of the acceleration time series (x), obtained using Fourier transform, plotted along with the theoretical spectrum computed using Eq.(2).

BRUNE'S FAR-FIELD MODEL

The amplitude spectrum of Brune's far-field model can be written as follows (Brune [5, 6]):

$$|A(\omega)| = \frac{2C_P R_{\theta\phi} M_0}{4\pi\beta^3\rho R} \frac{\omega^2}{(1+(\omega/\omega_c)^2)} \exp(-\tfrac{1}{2}\kappa\omega) \tag{6}$$

where M_0 is the seismic moment, $R_{\theta\phi}$ is the radiation pattern, C_p is a reduction factor accounting for the partitioning of the energy into two horizontal components, R is a function representing geometrical spreading, β is the shear-wave velocity, ω_c (= $2\pi f_c$) is the corner frequency, and ρ is the material density of the crust. The Brune's model is extended with en exponential term to account for the spectral decay at higher frequencies. Here it is assumed, as an engineering approximation, that the spectral decay parameter, $\kappa = R/Q\beta$ (Q is a path-averaged quality factor), increases very slowly within distance and is near constant within a certain radius of the earthquake source (Anderson [19]; Ólafsson [20]).

The corner frequency is defined as [5,6]

$$\omega_c = 2.34\beta/r_B \tag{7}$$

where r_B is the fault radius. The fault radius of a circular fault is given according to Brune [5, 6] as

$$r_B = (7M_0/16\Delta\sigma)^{1/3} \tag{8}$$

where Δσ denotes the stress drop. This is found as a reasonable approximation for the study area, at least for moderate-sized earthquakes (Ólafsson et al. [23]). Hence the corner frequency is assumed related to seismic moment and stress drop as follows:

$$\omega_c = 2.34(16/7)^{1/3}\beta\left\{\frac{\Delta\sigma}{M_0}\right\}^{1/3} \tag{9}$$

The impulse response for the low-pass part of Eq.(6) can be written as

$$h(t) = t\mathrm{e}^{-t} \quad \text{for} \quad t \geq 0 \tag{10}$$

The transfer function can be expressed as

$$H(\omega) = \frac{1}{(1+j\omega \mathrm{T_c}))^2} \tag{11}$$

and $j\omega\mathrm{T_c}$ is an imaginary component where $j = (-1)^{1/2}$ and $T_c = 1/\omega_c$.

The method chosen here to discretise $H(\omega)$ is the impulse-invariant approach (see [13]). Using this method, the discrete transfer function $H(z)$ becomes

$$H(z) = \frac{\alpha^2}{(1-\mathrm{e}^{-\alpha}z^{-1})^2} \tag{12}$$

$\alpha = T_S/T_c$. The digital filter or AR(2) model representing Eq.(6) is as follows:

$$x_1(k) = 2e^{-\alpha} x_1(k-1) - e^{-2\alpha} x_1(k-2) + \alpha^2 w(k) \tag{13}$$

The double differentiation in Eq.(6), $(j\omega)^2$, can be represented by the discrete transfer function

$$H_2(z) = (1 - z^{-1})^2 / T_S^2 \tag{14}$$

The corresponding filter can be written as follows (MA(2) filter):

$$x_2(k) = \frac{1}{T_S^2}(x_1(k) - 2x_1(k-1) + x_1(k-2)) \tag{15}$$

A time series with the same spectral characteristics as in Eq.(1) can be simulated by passing white noise sequence through the filter of Eq.(13) and using the output as input to the double differentiation filter represented by Eq.(15). The filters can also be merged into one filter, representing a ARMA(2,2) model. Examples of the output of the filters in Eq.(13) and Eq.(15) are shown in Figure 2.

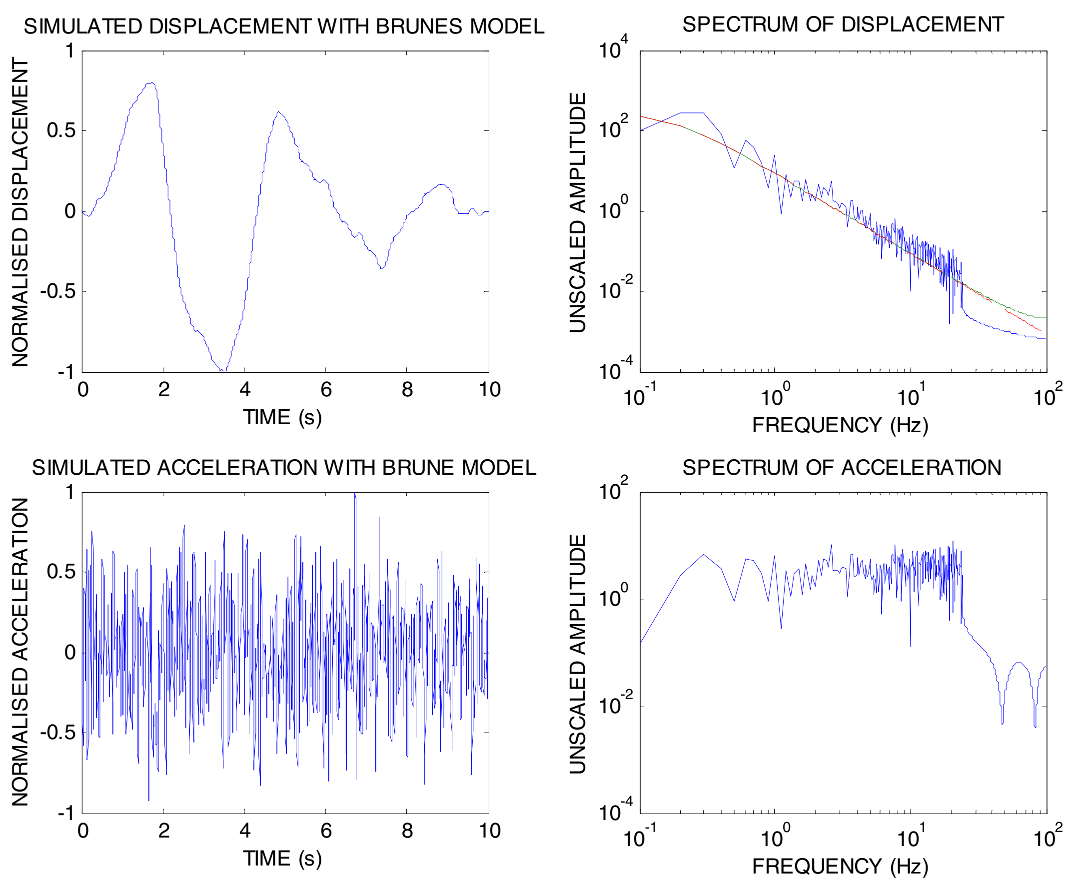

Figure 2: Simulation example. *Upper left*. Simulated displacement using Eq.(13). *Upper right*. Spectrum of displacement. *Lower left graph.* Acceleration simulated with Eqs.(13) and (15). *Lower right graph.* Fourier spectrum of simulated acceleration.

SPECTRAL DECAY FUNCTION

An additional filter is need to obtain the attenuation of high frequency components that is represented by the following function

$$H_3(\omega) = \mathrm{e}^{-\kappa\omega/2} \tag{16}$$

If $-\kappa\omega/2$ is small then a first order approximation can be applied to discretise Eq.(16) (see, for example, Safak [23]). Here, however, a use is made of the Fourier transform pair

$$H_3(\omega) = \mathrm{e}^{-\kappa\omega/2} \Leftrightarrow \frac{\kappa}{2\pi}\frac{1}{t^2 + (\kappa/2)^2} = h_3(t) \tag{17}$$

The discrete form of the transfer function $H_3(z)$ can be arrived at by z-transforming, the sampled version of $h_3(t)$, that is $h_3(t) = h_3(kT_S)$. This gives the following:

$$H_3(z) = \sum_{n=-\infty}^{\infty} h_3(n) z^{-n} = \sum_{n=-\infty}^{\infty} \frac{\kappa}{2\pi}\frac{z^{-n}}{\left(nT_S\right)^2 + \left(\kappa/2\right)^2} \tag{18}$$

The exponential function can therefore be realised by filter with the transfer function

$$H_3(z) = \sum_{n=1}^{2Np+1} h_3(n) z^{-n} \tag{19}$$

where N_p is the number of filter coefficients. Here the impulse response is

$$h(n) = \left[b_{N_p}, \ldots\ldots, b_2, b_1, b_0, b_1, b_2 \ldots., b_{N_p}\right] \tag{20}$$

and

$$b_i = \frac{\kappa}{2\pi}\frac{1}{\left(iT_S\right)^2 + (\kappa/2)^2} \qquad for \quad i = 1, 2, \ldots\ldots, N_p \tag{21}$$

The filter can be expressed as

$$x(k) = \sum_{n=1}^{2N_p+1} h(n) x_2(k-n) \tag{22}$$

The filter in Eq.(22) is a FIR filter where the infinite-duration impulse response is truncated. The filter also satisfies the condition $h(n) = h(N_p\text{-}1\text{-}n)$, which ensures a linear phase (see for example Oppenheimer [24]). This property of FIR filters is important for processing time-series (for example low-pass and band-pass filtering) where the preservation of the phase is important. An example of output from the spectral decay filter can be seen in Figure 3 when the input is white noise. The theoretical spectral attenuation (Eq.(16)) is also shown. Figure 3 also shows the application of the filter (Eq.(22)) to shape the high frequency of acceleration simulated with Brunes's model (Eqs (13) and (15)). A low-pass filter with cut-off frequency of 24 Hz is applied to band-limit the white noise driving sequence.

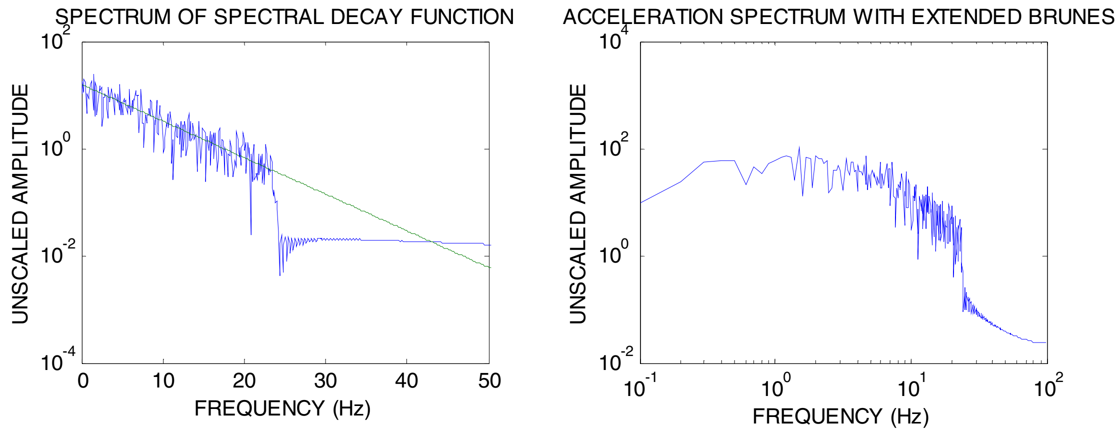

Figure 3: Effects of the spectral decay function. ***Graph on left.*** **Spectral decay filter (Eq.(22)) driven by a white noise sequence plotted along with Eq.(16).** ***Graph on right.*** **Spectral decay filter applied to acceleration simulated with Brune's model (Eqs. (13) and (15)).**

SITE AMPLIFICATION

A discrete time site amplification model for vertically propagating *S*-waves has been presented by Safak [23]. Here the model for a single soft layer over bedrock will be considered. The transfer function of the model, for large values of Q_0, is given as follows:

$$E(f) = \frac{(1+r)\mathrm{e}^{-j2\pi f\tau}\mathrm{e}^{-\pi f\tau/Q_0}}{1+r\mathrm{e}^{-j4\pi f\tau}\mathrm{e}^{-2\pi f\tau/Q_0}} \tag{23}$$

where r is the reflection coefficient at the junction of the soft layer and bedrock, τ is the travel time in the soft layer, Q_0 is the attenuation in the soil layer. The resonant peaks of the amplification are equally spaced at frequencies

$$f_{si} = i/(4\tau) \quad i = 1,3,5,\ldots. \tag{24}$$

Assuming a large value of Q_0, so that $1/(2Q_0) \approx 0$ is a reasonable approximation, the transfer function in Eq.(23) can be written in terms of $z = \exp(j2\pi f T_S)$, as

$$E(z) = \frac{(1+r)z^{-\tau/T_S}}{1+rz^{-2\tau/T_S}} \tag{25}$$

The discrete time model can be written as

$$x(k) = -rx(k-n) + (1+r)w(k-m) \tag{26}$$

where

$$n = \mathrm{round}(2\tau/T_S) \quad m = \mathrm{round}(\tau/T_S) \tag{27}$$

Figure 4 shows the amplitude of the site amplification transfer function, Eq.(25). Also shown is the simulated acceleration using Brune’s model, Eqs. (13), (15) and (22), as well as the site amplification filter, Eq. (26). Also shown is the Fourier transform of the simulated acceleration.

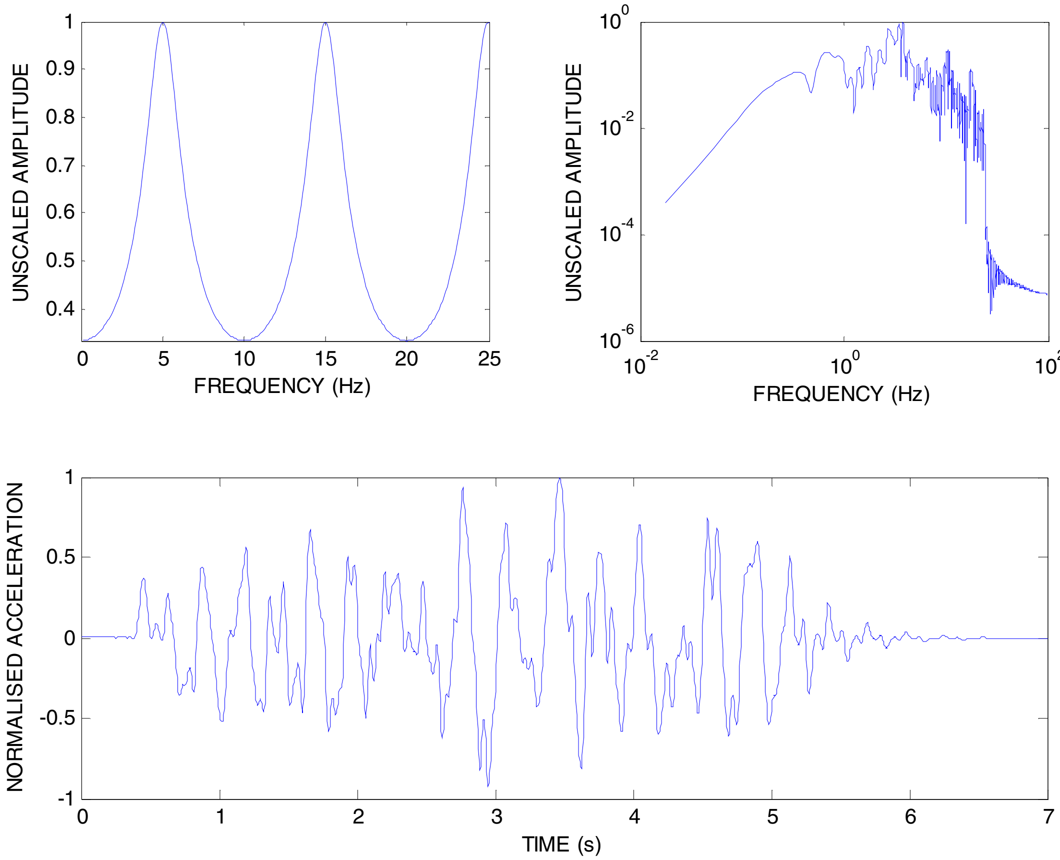

Figure 4: Site amplification. ***Upper left graph.*** **Amplitude of transfer function represented by Eq. (25).** ***Upper right graph.*** **Fourier transform of simulated acceleration.** ***Bottom graph.*** **Simulated acceleration using Eqs.(13), (15), (22) and (26).**

BRUNE’S NEAR-FIELD MODEL

The model in Eqs.(6) can be applied to far-field data. For short epicentral distances Brune’s near-field model is a better choice [5, 6]. The amplitude spectrum of Brune’s near-field model, extended with an exponential function, can be written as

$$\left|A(\omega)\right| = \frac{7}{8}\frac{C_p}{\rho\ \ \beta}\frac{M_0}{r_B^3}\frac{\omega}{\sqrt{\omega^2+\tau_R^{-2}}}\exp(-\frac{1}{2}\kappa_O\omega) \tag{28}$$

where κ_o is the spectral decay of the near-field spectra and τ_R is the so-called rise time. The following discrete time models can be applied to simulate time sequences with spectral characteristics described by the low-pass part and the differentiation in Eq.(28).

$$x_1(k) = \mathrm{e}^{-d} x_1(k-1) + d \cdot w(k) \tag{29}$$

$$x_2(k) = \frac{1}{T_\mathrm{S}}(x_1(k) - x_1(k-1)) \tag{30}$$

where $d = T_s/\tau$. The exponential term is accounted for by passing the output sequences that have passed through the filters of Eqs.(29) and (30), through a similar filter spectral decay as represented by Eq.(22).

SAVAGE-HASKELL MODEL

For an earthquake that can be approximated as a point source Brune's models are found to be good approximations for engineering purposes. For an earthquake on a fault where one dimension is much greater than the other and directivity is considered then the Haskell-Savage model can be applied (see Haskell [25] and Savage [26]. The amplitude of the acceleration spectrum is expressed as A second source model used in what follows is a model put forward by Savage [26] and is based on a theory by Haskell [25]. The amplitude displacement spectra for this model can be written as

$$\left|A(\omega)\right| = \frac{2C_\mathrm{p} R_{\theta\phi} M_0 \omega^2 F}{4\pi\beta^3 \rho R (1+\omega^2 {T_\mathrm{c}}^2)^{1/2}} \mathrm{e}^{-\kappa\omega/2} \tag{31}$$

where $T_\mathrm{c} = 1/(1.078\omega_\mathrm{c})$ and F is a directivity function of the rupture (see [26] or [27] for details).

The directivity function $F = F_1$, assuming a uni-lateral propagation, is written as follows:

$$F_1(\omega, \tau_0) = \frac{\sin(\omega\tau_0/2)}{\omega\tau_0/2} \tag{32}$$

with τ_0 defined by

$$\tau_0 = \frac{L((v_\mathrm{c}/v_\mathrm{r}) - \cos\theta)}{v_\mathrm{c}} \tag{33}$$

where v_c represents either α (*P*-wave velocity) or β (*S*-wave velocity). The parameters θ and ϕ are angles defining the direction from the source to the measurement site, v_r is the rupture velocity, and L is the length of the fault. For a bi-directional rupture the directivity $F(\omega,\tau_0,\tau_\mathrm{p})$ is represented by the following expression

$$\begin{aligned} F(\omega, \tau_0, \tau_\pi) \quad &= \{(L_0 F_1(\omega, \tau_0))^2 + (L_\pi F_1(\omega, \tau_\pi))^2 + 2 L_0 L_\pi F_1(\omega, \tau_0) F_1(\omega, \tau_\pi) \\ &\qquad - \cos(\omega(\tau_0 - \tau_\pi)/2)\}^{1/2} / (L_0 + L_\pi) \end{aligned} \tag{34}$$

where τ_0 is obtained as in Eq.(33) by replacing L with L_0 and τ_π is similarly obtained in a similar fashion by replacing L in Eq.(33) with L_π.

For finding the discrete representation of the sinc function in Eq.(32), the following relation can be used

$$\sin(\omega M_1) = \frac{z^{M_1} - z^{-M_1}}{2j} \tag{35}$$

By using $(1-z^{-1})^{-1}$ for the integrating factor, $(j\omega)^{-1}$, the discrete time transfer function can be written as

$$F_1(z) = \frac{1}{2M_1}\left\{\frac{z^{M_1} - z^{-M_1}}{1-z^{-1}}\right\} \tag{36}$$

where

$$M_1 = \text{round}(F_S\tau_0/2) \quad M_2 = \text{round}(F_S\tau_\pi/2) \tag{37}$$

Furthermore by using the following relation

$$2\cos(\omega B) = z^B + z^{-B} \tag{38}$$

where $B = (\tau_0-\tau_p)/2T_S$, the discretised function $F(z)$ can be written as follows:

$$F(z) = \left\{\frac{1}{L_0 + L_\pi}\right\}\left\{\left\{\frac{L_0}{2M_1}\right\}\frac{\left(z^{M_1} - z^{-M_1}\right)}{(1-z^{-1})} + \left\{\frac{L_\pi}{2M_2}\right\}\frac{\left(z^{M_2} - z^{-M_2}\right)}{(1-z^{-1})}z^B\right\} \tag{39}$$

where

$$M_1 = \text{round}(F_S\tau_0/2) \quad M_2 = \text{round}(F_S\tau_\pi/2) \quad B = (\tau_0 - \tau_\pi)/(2T_S) \tag{40}$$

The low-pass part of the transfer function $A(\omega)$ in Eq. (31) can be written as

$$H_0(\omega) = \frac{1}{1 + j\omega T_c} \tag{41}$$

and can be represented by the following discrete transfer function

$$H_0(z) = \frac{a}{1 - e^{-a}z^{-1}} \tag{42}$$

where $a = T_S/T_c$. This can be realised by the discrete time equation

$$x_1(k) = e^{-a}x_1(k-1) + aw(k) \tag{43}$$

The following recursive equation represents the directivity function of Eq.(34)

$$\begin{aligned} x_2(k) = {} & x_2(k-1) + A_1x_1(k+M_1) + B_1x_1(k+M_2+B) \\ & - A_1x_1(k-M_1) - B_1x_1(k-M_2+B) \end{aligned} \tag{44}$$

where $A_1 = L_0/2M_1$, and $B_1 = L_\pi/2M_2$.

The transfer function amplitudes of the continuous model (Eq. (34)) and the average Fourier spectrum of 10 simulation runs (N = 4000, T_S = 0.01, N_p = 120) using the discrete model were compared and the results are shown in Figure 5. The parameters used were v_r, L_0 and L_π.

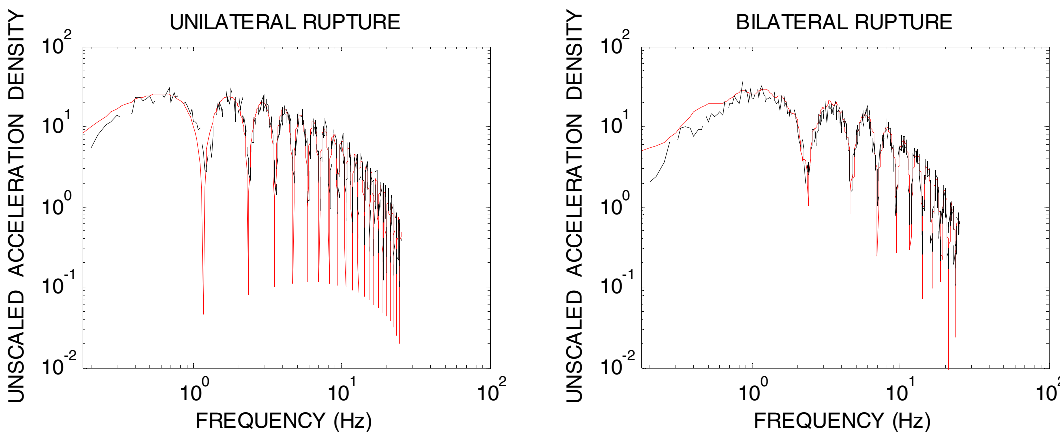

Figure 5: The Savage-Haskell model. The solid curve represents the theoretical model of Eq.(31) but the dashed line represents the average Fourier spectrum of x acceleration sequences simulated with Eq.(44). ***Left graph.*** **Unilateral rupture.** ***Right graph.*** **Bi-lateral rupture.**

RESPONSE SPECTRUM MODELS

The displacement response spectra are defined as the maximum value of the response of a second-order system subjected to a subjected to earthquake motions $a(t)$, at a certain undamped natural frequency ω_0, and damping ratio ζ, that is

$$S_d(\omega_0, \zeta) = |y(t)|_{\max} \tag{45}$$

The second-order system in Figure can be described by the following equation (see, for instance, Clough[28] or Langen and Sigbjörnsson [29])

$$\ddot{y}(t) + 2\zeta\omega_0\dot{y}(t) + \omega_0^2 y(t) = -a(t) \tag{46}$$

where $y(t)$ is the relative displacement of the mass m with respect to the ground, is the undamped natural frequency, and $\zeta = c/2m\omega_0$ is a fraction of critical damping. The general solution of Eq.(46) is

$$y(t) = -\int_0^t a(\tau)h(t-\tau)d\tau \tag{47}$$

where $h(t)$ is the impulse response of the system and is written as

$$h(t) = \begin{cases} \dfrac{1}{\omega_\mathrm{d}} \mathrm{e}^{-\omega_0 \zeta t} \sin(\omega_\mathrm{d} t) & t \geq 0 \\ 0 & t < 0 \end{cases} \tag{48}$$

where ω_d is the damped natural frequency and can be expressed as follows:

$$\omega_\mathrm{d} = \omega_0 \sqrt{1-\zeta^2} \tag{49}$$

The discretised impulse response can be written as

$$h(kT_\mathrm{S}) = \begin{cases} \dfrac{1}{\omega_\mathrm{d}} \mathrm{e}^{-k\omega_0 \zeta T_\mathrm{S}} \sin(\omega_\mathrm{d} kT_\mathrm{S}) & t \geq 0 \\ 0 & t < 0 \end{cases} \tag{50}$$

The discretised transfer function, $H(z)$, of the system in Eq. (50) can be obtained using the z-transform and can be written as follows.

$$H(z) = \frac{1}{\omega_\mathrm{d}} \frac{\mathrm{e}^{-\zeta\omega_0 T_S} \sin(\omega_\mathrm{d} T_\mathrm{S}) z^{-1}}{1 - 2\mathrm{e}^{-\zeta\omega_0 T_\mathrm{S}} \cos(\omega_\mathrm{d} T_\mathrm{S}) z^{-1} + \mathrm{e}^{-2\zeta\omega_0 T_\mathrm{S}} z^{-2}} \tag{51}$$

A filter for the displacement response determined from the transfer function $H(z)$ of Eq. (51) is written as follows:

$$\begin{aligned} y(k) = {} & 2\mathrm{e}^{-\zeta\omega_0 T_S} \cos(\omega_\mathrm{d} T_\mathrm{S}) y(k-1) - \mathrm{e}^{-2\zeta\omega_0 T_\mathrm{S}} y(k-2) \\ & - \frac{\mathrm{e}^{-\zeta\omega_0 T_\mathrm{S}} \sin(\omega_\mathrm{d} T_\mathrm{S})}{\omega_\mathrm{d}} a(k-1) \end{aligned} \tag{52}$$

The transfer function can also be obtained from the autocorrelation function. Similarly filters for computing the velocity- and acceleration-response can be realised.

The velocity response spectra can be expressed as (Hudson [30]):

$$S_\mathrm{v}(\omega_0, \zeta) = |\dot{y}(t)|_{\max} = \left[-\int_0^t a(u) \mathrm{e}^{-\omega_0 \zeta (t-u)} \cos(\omega_\mathrm{d}(t-u)) du + \frac{\zeta}{\sqrt{1-\zeta^2}} \int_0^t a(u) \mathrm{e}^{-\omega_0 \zeta (t-u)} \sin(\omega_\mathrm{d}(t-u)) du \right]_{\max} \tag{53}$$

The discretised impulse reponse for the first term in Eq.(53), can be expressed as

$$h_1(kT_\mathrm{S}) = \begin{cases} \mathrm{e}^{-k\omega_0 \zeta T_\mathrm{S}} \cos(\omega_\mathrm{d} kT_\mathrm{S}) & t \geq 0 \\ 0 & t < 0 \end{cases} \tag{54}$$

The discrete transfer function $H_1(z)$ can be written as

$$H_1(z) = \frac{1 - \mathrm{e}^{-\zeta\omega_0 T_\mathrm{S}} \cos(\omega_\mathrm{d} T_\mathrm{S}) z^{-1}}{1 - 2\mathrm{e}^{-\zeta\omega_0 T_\mathrm{S}} \cos(\omega_\mathrm{d} T_\mathrm{S}) z^{-1} + \mathrm{e}^{-2\zeta\omega_0 T_\mathrm{S}} z^{-2}} \tag{55}$$

The recursive discrete time equation for the velocity response, $y_v(k)$, can now be written as

$$\begin{aligned} y_{\mathrm{v}}(k) &= 2\mathrm{e}^{-\zeta\omega_0 T_S}\cos(\omega_{\mathrm{d}}T_{\mathrm{S}})\,y_{\mathrm{v}}(k-1) - \mathrm{e}^{-2\zeta\omega_0 T_S}\,y_{\mathrm{v}}(k-2) - a(k) \\ &\quad + \left(\mathrm{e}^{-\zeta\omega_0 T_S}\cos(\omega_{\mathrm{d}}T_{\mathrm{S}}) + \frac{\zeta}{\sqrt{1-\zeta^2}}\mathrm{e}^{-\zeta\omega_0 T_S}\sin(\omega_{\mathrm{d}}T_{\mathrm{S}})\right)a(k-1) \end{aligned} \tag{55}$$

The recursive Eq.(55) was used to compute the velocity response spectra for 10 accelerograms that were simulated with Brune's model. The results are shown in Figure 6 (left graph). The solid (red) curve represents one the spectrum for one realisation and the dashed (blue) curve represent the average of the 10 realisations. In the graph on the right hand side of Figure 6 the results from the computation of the velocity response of the 10 simulations using the ARMA(4,1) of Eq.(5).

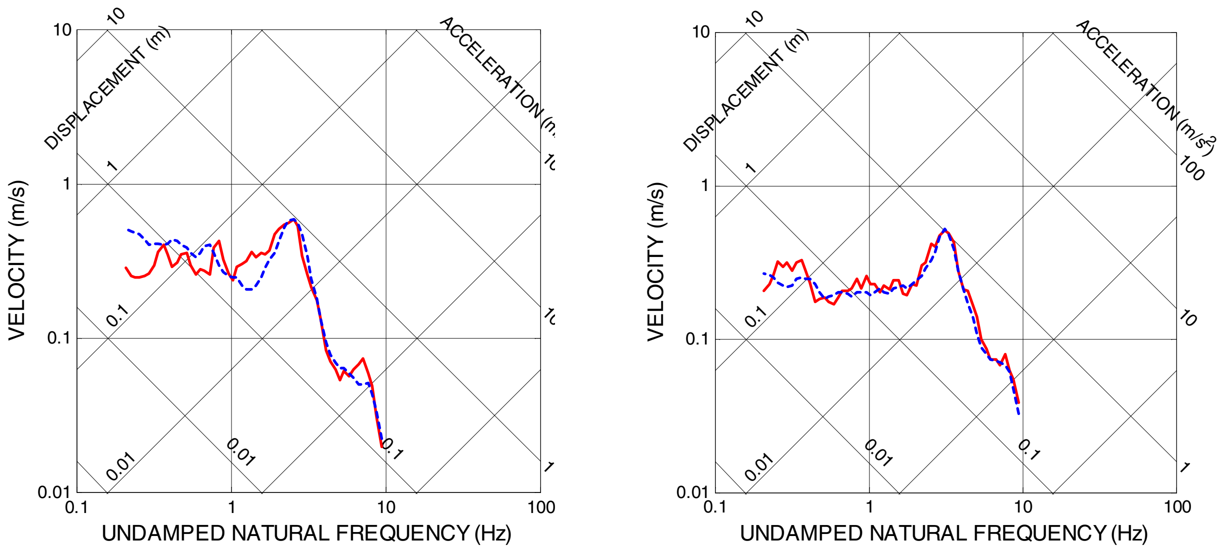

Figure 6: Velocity response spectra of 10 accelerograms simulated using. *Graph on left.* Brune's model. *Graph on right.* ARMA(4,1) model of Eq.(5). The solid (red) curve represents the spectrum for one realisation and the dashed (blue) curve represent the average of the 10 realisations.

DISCUSSION

The discrete time series models are either based on models that have some physical meaning as in the case of the models that are considered in this paper for ground motion modelling. Another approach is the so-called black-box approach where no attempt is made to attach physical meaning to the parameters.

The discrete time counterparts of the strong-motion models that are formulated in continuous time are derived here. The resulting filter equations that can be used for simulation have not been scaled so that the variance of the output is the same as the variance of the input signal. The scaling can be done by integrating the transfer function of the filter and using the result as a normalising factor. Usually the output variance from these models is normalised afterwards and scaled with respect to pga or rms-acceleration obtained from attenuation relations.

Using discrete time models has some clear advantages. These advantages have made them extremely popular for modelling and estimation in control, signal processing and system identification. Once you have the parameters the simulation is extremely straightforward. It is just a matter of passing a noise sequence through recursive filter equations. Another advantage is link between the recursive filter equations and the discrete transfer function. This means that when the parameters are known then the transfer function can also be determined using the parameters. The parametric time series models have also advantages as consistent spectral estimator as compared with the classical periodogram where the bias decreases but not the variance with added information.

The main disadvantages are for example the order determination problem for black box models and also the parameter estimation algorithms for determining ARMA parameters usually require non-linear optimisation. This means somewhat more complex estimation algorithms as opposed to simply applying the FFT. For the discrete time models there is a trade-off between model complexity or entropy and lowering the variance. The models are also bound by the limitations that digital filters in general have such as round-off noise and quantization effects.

CONCLUSIONS

This paper demonstrates the use of parametric time series models for simulating strong-ground motion and structural response. It is demonstrated that a discrete time counterpart of models that are formulated in continuous time can be conveniently obtained. Once the discrete time counterparts have been derived then filter with parameters that have physical meaning can be easily applied for simulating ground-motion.

ACKNOWLEDGEMENT

The work presented herein was supported by a grant from the University of Iceland Research Fund.

REFERENCES

1. Housner GW. “Properties of strong ground motion earthquakes”, Bulletin of the Seismological Society of America 1955; 45: 187-218.
2. Tajimi H. “A statistical method of determining the maximum response of building structure during an earthquake” Proceedings of the 2nd World Conference on Earthquake Engineering **2**, Japan, 1960.
3. Hanks TC and McGuire RK. “The character of high-frequency strong ground motion.” Bulletin of the Seismological Society of America 1981; 71: 2071-2095.
4. Boore DM. “Stochastic simulation of high-frequency ground motion based on seismological models of the radiated spectra.” Bulletin of the Seismological Society of America 1983; 73: 1865-1894. Brune J. “Tectonic stress and the spectra of shear waves from earthquakes.” Journal of Geophysical Research 1970; 75: 4997-5009.
5. Brune J. “Correction.” Journal of Geophysical Research 1971; 76: 5002.
6. Boore DM. “Simulation of Ground Motion Using the Stochastic Method.” Pure and Applied Geophysics 2003; 160: 635-676.
7. Chang MK, Kwiatkowski JW, Nau RF, Oliver RM, and Pister KS.“ARMA models for earthquake ground motions”, Earthquake Engineering and Structural Dynamics 1982; 10: 651-662.
8. Conte JP, Pister KS and Mahin SA. “Non-stationary ARMA modelling of seismic motions.” Soil Dynamics and Earthquake Engineering 1992; 11: 411-426.
9. Ólafsson S and Sigbjörnsson R. “Application of ARMA models to estimate earthquake ground motion and structural response.” Earthquake Engineering and Structural Dynamics 1995; 24: 951-966.
10. Imai H, Yun CB, Maruyama O and Shinozuka M. “Fundamentals of system identification in structural dynamics.” Probabilistic Engineering Mechanics 1989; 4: 162-173.

11. Celebi M and Safak E. “Seismic response of Transamerica Building.” Journal of Structural Engineering 1991; 117: 2389-2425.
12. Rabiner L and Gold B. “Theory & Application of Digital Signal Processing.” Prentice-Hall, 1975.
13. Marple L. “Digital Spectral Analysis with Applications.” Prentice Hall, 1987.
14. Ljung L. “System Identification: Theory for the user.” Prentice-Hall, 1987.
15. Haykin S. “Adaptive Filter Theory.” Prentice-Hall, 1986.
16. Ljung, L. “System Identification Toolbox, For Use with MATLAB, Users Guide, Version 5.” The Mathworks, Inc., 2001.
17. Swami A, Mendel JM and Crysostomos LN. “Higher-Order Spectral Analysis Toolbox, Users Guide, Version 2.” United Systems and Signals, Inc., 1993.
18. Chrysostomos LN and Athina PP. “Higher-Order Spectra Analysis, A Nonlinear Signal Processing Framework.” Prentice-Hall, 1993.
19. Ólafsson S. “Estimation of earthquake-induced response.” Department of Structural Engineering, Norwegian University of Science and Technology, Trondheim, 1999.
20. Anderson JG and Hough SE. “A model for the shape of the Fourier amplitude spectrum of acceleration at high frequencies.” Bulletin of the Seismological Society of America 1984; 74: 1969-1993.
21. Ólafsson S and Sigbjörnsson R. “A theoretical attenuation model for earthquake-induced ground motion”, Journal of Earthquake Engineering 1999, Imperial College Press; 3: 287-315.
22. Ólafsson S, Sigbjörnsson R and Einarsson P. (1998), “Estimation of Source Parameters and Q from Acceleration Recorded in the Vatnafjöll Earthquake in South Iceland.” Bulletin of the Seismological Society of America 1998; 88: 556-563.
23. Safak E. “Discrete-time analysis of seismic site amplification.” Journal of Engineering Mechanics 1995, ASCE, 121: 801-809.
24. Oppenheimer AV and Schafer RW. “Digital Signal Processing.” Prentice-Hall, 1975.
25. Haskell N. “Total energy and energy spectral density of elastic wave radiation from propagating faults.” Bulletin of the Seismological Society of America 1964; 54: 1811-1842.
26. Savage JC. “Relation of corner frequency to fault dimensions.” Journal of Geophysical Research 1972; 77: 3788-3795.
27. Kasahara K. “Earthquake Mechanics.” Cambridge University press, 1981.
28. Clough RW and Penzien J. “Dynamics of Structures 1993, second edition.” McGraw-Hill, 1993.
29. Langen I and Sigbjörnsson R. “Dynamic analysis of structures.” Tapir, 1979.
30. Hudson DE. “Reading and Interpreting Strong Motion Accelerograms.” Monograph Series, Earthquake Eng. Res. Institute, 262 Telegraph Ave., Berkeley, California, U.S.A, 1979.